

This is a repository copy of *What effect does VOC sampling time have on derived OH reactivity?*.

White Rose Research Online URL for this paper:

<https://eprints.whiterose.ac.uk/137793/>

Version: Submitted Version

---

**Article:**

Sonderfeld, H., White, I. R., Goodall, I. C. A. et al. (4 more authors) (2016) What effect does VOC sampling time have on derived OH reactivity? *Atmospheric Chemistry and Physics*. 6303–6318. ISSN 1680-7324

<https://doi.org/10.5194/acp-16-6303-2016>

---

**Reuse**

This article is distributed under the terms of the Creative Commons Attribution (CC BY) licence. This licence allows you to distribute, remix, tweak, and build upon the work, even commercially, as long as you credit the authors for the original work. More information and the full terms of the licence here:

<https://creativecommons.org/licenses/>

**Takedown**

If you consider content in White Rose Research Online to be in breach of UK law, please notify us by emailing [eprints@whiterose.ac.uk](mailto:eprints@whiterose.ac.uk) including the URL of the record and the reason for the withdrawal request.



1 **What effect does VOC sampling time have on derived OH**  
2 **reactivity?**

3

4 **H. Sonderfeld<sup>1</sup>, I.R. White<sup>1</sup>, I.C.A. Goodall<sup>1</sup>, J.R. Hopkins<sup>2</sup>, A.C. Lewis<sup>2</sup>, R.**  
5 **Koppmann<sup>3</sup>, P.S. Monks<sup>1</sup>**

6 [1]{Department of Chemistry, University of Leicester, Leicester, LE1 7RH, UK}

7 [2]{National Centre for Atmospheric Science, University of York, York, YO10 5DD, UK}

8 [3]{Institute for Atmospheric and Environmental Research, University of Wuppertal, 42119  
9 Wuppertal, Germany}

10 Correspondence to: P.S. Monks (P.S.Monks@leicester.ac.uk)

11

12 **Abstract**

13 State of the art techniques allow for rapid measurements of total OH reactivity. Unknown  
14 sinks of OH and oxidation processes in the atmosphere have been attributed to what has been  
15 termed ‘missing’ OH reactivity. Often overlooked are the differences in timescales over  
16 which the diverse measurement techniques operate. Volatile organic compounds (VOC)  
17 acting as sinks of OH are often measured by gas chromatography (GC) methods which  
18 provide low frequency measurements on a timescale of hours, while sampling times are  
19 generally only a few minutes. Here, the effect of the sampling time and thus the contribution  
20 of unmeasured VOC variability on OH reactivity is investigated. Measurements of VOC  
21 mixing ratios by proton transfer reaction time-of-flight mass spectrometry (PTR-ToF-MS)  
22 conducted during two field campaigns (ClearfLo and PARADE) in an urban and a semi-rural  
23 environment were used to calculate OH reactivity. VOC were selected to represent variability  
24 for different compound classes. Data were averaged over different time intervals to simulate  
25 lower time resolutions and were then compared to the mean hourly OH reactivity. The results  
26 show deviations in the range of 1 to 25%. The observed impact of VOC variability is found  
27 to be greater for the semi-rural site.

28 The selected compounds were scaled by the contribution of their compound class to the total  
29 OH reactivity from VOC based on concurrent gas chromatography measurements conducted



1 during the ClearfLo campaign. Prior to being scaled, the variable signal of aromatic  
2 compounds results in larger deviations in OH reactivity for short sampling intervals compared  
3 to oxygenated VOC (OVOC). However, once scaled with their lower share during the  
4 ClearfLo campaign this effect was reduced. No seasonal effect on the OH reactivity  
5 distribution across different VOC was observed at the urban site.

6

## 7 **1 Introduction**

8 Atmospheric photochemistry produces a variety of radicals that exert a substantial influence  
9 on the ultimate composition of the atmosphere. The OH radical is the main oxidant in the  
10 atmosphere (Monks et al., 2009 and references therein). Its actual concentration being  
11 determined by the balance between its sources and sinks. While in many cases OH sources are  
12 well understood, its sinks are manifold and not completely characterised. OH reactivity is a  
13 measure of the strength of the sinks for the OH radical. It can be derived from the reaction  
14 rates of the reactants  $k_{OH+X}$  and their concentrations  $[X]$  (Kovacs et al., 2003):

$$15 \quad k_{OH} = \sum k_{OH+VOC_i} [VOC_i] + k_{OH+CO} [CO] + k_{OH+NO} [NO] + k_{OH+NO_2} [NO_2] + k_{OH+SO_2} [SO_2] + \dots \quad (1)$$

16 In-situ measurements of OH reactivity have provided new insights into OH loss chemistry  
17 and the oxidative ability of the atmosphere (Di Carlo et al., 2004; Edwards et al.,  
18 2013; Hofzumahaus et al., 2009; Whalley et al., 2011; Yoshino et al., 2006). There are a  
19 number of different techniques used for the direct measurement of OH reactivity. The total  
20 OH loss rate measurement technique (TOHLM) was one of the first techniques applied for  
21 determination of total OH reactivity based on a single measurement (Ingham et al., 2009; Ren  
22 et al., 2003a; Shirley et al., 2006). TOHLM is based on the measurement of the decay of  
23 artificially produced OH following the introduction of reactants into an ambient air sample  
24 within a flow tube. By varying the distance between the OH injection point and the detector,  
25 the reaction time changes and provides a series of relative decay rates (Kovacs and Brune,  
26 2001; Kovacs et al., 2003). A similar approach is taken with the laser-induced pump and probe  
27 technique, whereby decay in OH is detected by time-resolved laser-induced fluorescence  
28 (Sadanaga et al., 2004). Another technique developed by Sinha et al. (2008) called  
29 Comparative Reactivity Method (CRM) is based on the measurement of a single reactant  
30 (most often pyrrole) which first reacts with OH under clean air conditions and then under  
31 competitive conditions with ambient air. The reaction takes place in a glass vessel and is most



1 commonly probed by PTR-MS. Recently, Nölscher et al. (2012b) presented a GC-PID for the  
2 detection of pyrrole for CRM.

3 These techniques enable comparison of directly measured OH reactivity to calculated OH  
4 reactivity using equation (1) based on measurements of individual compounds. The difference  
5 between the two, is being referred to as missing OH reactivity. Reasons for an under  
6 prediction of OH reactivity maybe due to incomplete or inaccurate measurements of  
7 individual compounds (Di Carlo et al., 2004;Kim et al., 2011;Kovacs and Brune, 2001).  
8 Therefore, direct measurements of total OH reactivity can help to evaluate the completeness  
9 of measured VOC budgets (Dolgorouky et al., 2012;Mao et al., 2009;Mogensen et al., 2011).

10 In urban environments good agreement between measured and calculated OH reactivity have  
11 been found. For example, no significant missing OH reactivity was found in New York during  
12 summer (Ren et al., 2003b) and for both Paris under clean marine air conditions (Dolgorouky  
13 et al., 2012) and Tokyo (Yoshino et al., 2006) in the winter. Larger missing OH reactivity of  
14 up to 30% was found for all other seasons in Tokyo by Yoshino et al. (2006), presumably  
15 owing to secondary reaction products, including semi volatile oxygenated compounds, from  
16 atmospheric oxidation of VOC. A similar amount of missing OH reactivity was reported by  
17 Kovacs et al. (2003) for urban measurements in Nashville. They suggest that non measured  
18 short lived VOC accounted for the missing reactivity. In Paris, a missing OH reactivity of up  
19 to 75% was found for continentally influenced air, which is also attributed to highly oxidized  
20 compounds from photochemical processes during transportation of these air masses  
21 (Dolgorouky et al., 2012). Similar reasons were reported by Lou et al. (2010) to account for  
22 missing OH reactivity measured in the highly populated Pearl River Delta.

23 Direct measurements of OH reactivity in rural areas generally tend to have larger missing OH  
24 reactivity. Using PTR-MS and the CRM method in a boreal forest in Finland during August  
25 2008, Sinha et al. (2010) reported missing OH reactivity of approximately 50%. This site was  
26 revisited in 2010, when missing OH reactivity of 58% to 89% was recorded (Nölscher et al.,  
27 2012a). Similar results in a mixed deciduous forest where obtained by Hansen et al. (2014)  
28 who reported missing OH reactivity of 46% to 65%. Both studies concluded that unmeasured  
29 oxidation products were missing from the OH reactivity calculation. In contrast to those  
30 findings, Ren et al. (2006) found no significant missing OH reactivity on average during a  
31 summertime campaign in a deciduous forest in New York in 2002. They attributed this to  
32 differences in the composition of emitted biogenic VOC (BVOC). Rainforests are a large



1 sink for OH as they emit a huge amount of VOC. Measured OH reactivity in the rainforest of  
2 Borneo during April 2008 yielded a missing OH reactivity of 70% compared to calculated  
3 reactivity from measurements of single compounds (Edwards et al., 2013) and ~53%  
4 compared to modelled reactivity (Whalley et al., 2011). Since isoprene makes up the biggest  
5 contribution to OH reactivity the effect of oxidation products of isoprene were discussed  
6 (Edwards et al., 2013; Whalley et al., 2011).

7 While different possible explanations for missing OH reactivity have been given, the wide  
8 range in reported missing OH reactivity suggests that many reactants and processes remain  
9 unknown or cannot be measured at present. Measurements of total non-methane organic  
10 carbon in the West Los Angeles Basin (Chung et al., 2003) and results following the  
11 application of a double-column (orthogonal) GC for urban air measurements (Lewis et al.,  
12 2000) emphasize the large number of OH reactants that are not measured with standard field  
13 equipment.

14 Measurements of non methane hydrocarbons (NMHC) used for calculation of OH reactivity  
15 are often performed with GC (Lou et al., 2010; Sadanaga et al., 2005; Shirley et al., 2006) and  
16 therefore the time resolution of the calculated OH reactivity is low due to sample run times up  
17 to 90 min (Dolgorouky et al., 2012), when compared to measured total OH reactivity.  
18 However, the sampling time during one GC cycle is shorter than the analysis time and thus,  
19 any high temporal variability in measured OH reactivity is not easily captured when it is  
20 derived from GC data (Nölscher et al., 2012a). When measured and calculated OH reactivity  
21 are compared, high time resolution data are often averaged over intervals that correspond to  
22 the GC cycle.

23 This work addresses the question of how temporal VOC concentration variability is reflected  
24 with different sampling time resolutions. Furthermore, the effect of averaging VOC data on  
25 calculated OH reactivity is discussed alongside how this may affect the amount of so called  
26 `missing` OH reactivity.

27 Relatively high time resolved VOC data collected by PTR-ToF-MS are used to calculate OH  
28 reactivity for selected compounds. Differing time resolutions are analysed to explore the  
29 effects. Data from an urban winter campaign are compared to measurements from a semi-  
30 rural summer campaign.

31



## 1 **2 Experimental section**

2 Two different sets of VOC mixing ratios measured with PTR-ToF-MS were used for analysis.  
3 One was collected during the ClearfLo (Clean Air for London, [www.clearflo.ac.uk](http://www.clearflo.ac.uk))  
4 (Bohnenstengel et al., 2015) winter campaign in 2012 at an urban background site in London,  
5 UK. The second was taken during the PARADE (PARTicles and RADicals: Diel observations  
6 of the impact of urban and biogenic Emissions, <http://parade2011.mpich.de/>) campaign in late  
7 summer 2011 at a semi-rural site located in the Taunus ridge, Germany.

### 8 **2.1 Field data**

9 **ClearfLo.** A PTR-ToF-MS (Series I; Kore Technology Ltd., UK) (Barber et al.,  
10 2012;Thalman et al., 2014) was deployed at Sion Manning School (51°31'15" N, 0°12'51"  
11 W) nearby the North Kensington urban background station in London during the intensive  
12 observation periods of the ClearfLo project in 2012. A general overview of the ClearfLo  
13 project and the measurement site is given in (Bohnenstengel et al., 2015). For background  
14 measurements a hydrocarbon trap was employed. Calibration measurements were performed  
15 before the campaign. For the calibration of toluene and xylene a permeation tube was used  
16 and calibration of acetone was done with Tedlar bags containing different dilutions of an  
17 acetone standard. The stability of the instrument during the campaign was monitored with a  
18 bromobenzene internal standard. Of the two intensive observation periods (IOP) (i.e., winter:  
19 6 January to 11 February and summer: 21 July to 23 August) data from 1 to 7 February 2012  
20 were selected for analysis in this study. During this period the measurement site was  
21 influenced by local sources, as well as by air masses from other parts of the UK and the  
22 continent (Bohnenstengel et al., 2015).

23 A dual channel GC with flame ionisation detector (DC-GC-FID; Hopkins et al. (2003)) was  
24 deployed at the same site as the PTR-ToF-MS during the ClearfLo IOPs. A wide range of  
25 VOC including alkanes, alkenes, dienes, aromatic compounds and OVOC was measured (see  
26 Table 1). The sampling time was 10 min while the analysis runtime was around 50 min,  
27 resulting in approximately one measurement per hour.

28



- 1 Table 1: Mixing ratios, rate coefficient and OH reactivity of the VOC measured with DC-GC-
- 2 FID during ClearfLo from 1 – 7 February 2012.

Compound	VMR (ppbV)	Concentration (molecules cm <sup>-3</sup> )	k <sub>OH</sub> (cm <sup>3</sup> molecules <sup>-1</sup> s <sup>-1</sup> )	OH reactivity (s <sup>-1</sup> )
<b>Alkanes</b>				
Ethane <sup>a</sup>	12.91 ± 10.89	(3.14 ± 2.65) × 10 <sup>11</sup>	2.40 × 10 <sup>-13</sup>	0.075
Propane <sup>a</sup>	4.59 ± 3.35	(1.12 ± 0.81) × 10 <sup>11</sup>	1.10 × 10 <sup>-12</sup>	0.123
iso-Butane <sup>b</sup>	1.42 ± 1.00	(3.45 ± 2.43) × 10 <sup>10</sup>	2.12 × 10 <sup>-12</sup>	0.073
n-Butane <sup>b</sup>	2.35 ± 1.60	(5.71 ± 3.89) × 10 <sup>10</sup>	2.36 × 10 <sup>-12</sup>	0.135
Cyclopentane <sup>b</sup>	0.10 ± 0.11	(2.50 ± 2.58) × 10 <sup>9</sup>	4.97 × 10 <sup>-12</sup>	0.012
iso-Pentane <sup>b</sup>	0.83 ± 0.62	(2.03 ± 1.50) × 10 <sup>10</sup>	3.60 × 10 <sup>-12</sup>	0.073
n-Pentane <sup>b</sup>	0.42 ± 0.26	(1.02 ± 0.64) × 10 <sup>10</sup>	3.80 × 10 <sup>-12</sup>	0.039
2,3-Methylpentane <sup>b*</sup>	0.35 ± 0.29	(8.56 ± 6.93) × 10 <sup>9</sup>	3.10 × 10 <sup>-11</sup>	0.265
n-Hexane <sup>b</sup>	0.13 ± 0.09	(3.16 ± 2.29) × 10 <sup>9</sup>	5.20 × 10 <sup>-12</sup>	0.016
n-Heptane <sup>b</sup>	0.09 ± 0.07	(2.18 ± 1.58) × 10 <sup>9</sup>	6.76 × 10 <sup>-12</sup>	0.015
2,2,4 TMP <sup>b</sup>	0.04 ± 0.02	(9.88 ± 5.22) × 10 <sup>8</sup>	3.34 × 10 <sup>-12</sup>	0.003
n-Octane <sup>b</sup>	0.03 ± 0.02	(6.75 ± 3.75) × 10 <sup>8</sup>	8.11 × 10 <sup>-12</sup>	0.005
<b>Alkenes</b>				
Ethene <sup>a</sup>	1.93 ± 1.04	(4.68 ± 2.52) × 10 <sup>10</sup>	7.80 × 10 <sup>-12</sup>	0.365
Propene <sup>a</sup>	0.43 ± 0.30	(1.05 ± 0.73) × 10 <sup>10</sup>	2.90 × 10 <sup>-11</sup>	0.306
trans-2-Butene <sup>b</sup>	0.04 ± 0.03	(1.03 ± 0.81) × 10 <sup>9</sup>	6.40 × 10 <sup>-11</sup>	0.066
1-Butene <sup>b</sup>	0.08 ± 0.05	(1.90 ± 1.21) × 10 <sup>9</sup>	3.14 × 10 <sup>-11</sup>	0.060
iso-Butene <sup>a</sup>	0.11 ± 0.07	(2.63 ± 1.77) × 10 <sup>9</sup>	5.10 × 10 <sup>-11</sup>	0.134
cis-2-Butene <sup>b</sup>	0.03 ± 0.02	(6.92 ± 5.72) × 10 <sup>8</sup>	5.64 × 10 <sup>-11</sup>	0.039
trans-2-Pentene <sup>b</sup>	0.04 ± 0.03	(9.13 ± 7.37) × 10 <sup>8</sup>	6.70 × 10 <sup>-11</sup>	0.061
1-Pentene <sup>b</sup>	0.03 ± 0.02	(7.32 ± 5.27) × 10 <sup>8</sup>	3.14 × 10 <sup>-11</sup>	0.023
Acetylene <sup>a</sup>	1.43 ± 0.74	(3.47 ± 1.81) × 10 <sup>10</sup>	7.50 × 10 <sup>-13</sup>	0.026
<b>Dienes</b>				
Propadiene <sup>b</sup>	0.02 ± 0.01	(4.40 ± 2.61) × 10 <sup>8</sup>	9.82 × 10 <sup>-12</sup>	0.004
1,3-Butadiene <sup>b</sup>	0.05 ± 0.03	(1.14 ± 0.76) × 10 <sup>9</sup>	6.66 × 10 <sup>-11</sup>	0.076
Isoprene <sup>a</sup>	0.02 ± 0.02	(5.37 ± 4.07) × 10 <sup>8</sup>	1.00 × 10 <sup>-10</sup>	0.054
<b>Aromatic compounds</b>				
Benzene <sup>a</sup>	0.41 ± 0.17	(9.88 ± 4.06) × 10 <sup>9</sup>	1.20 × 10 <sup>-12</sup>	0.012
Toluene <sup>a</sup>	0.64 ± 0.48	(1.56 ± 1.17) × 10 <sup>10</sup>	5.60 × 10 <sup>-12</sup>	0.087
Ethylbenzene <sup>b</sup>	0.14 ± 0.11	(3.48 ± 2.57) × 10 <sup>9</sup>	7.00 × 10 <sup>-12</sup>	0.024
m+p Xylene <sup>b*</sup>	0.18 ± 0.14	(4.28 ± 3.52) × 10 <sup>9</sup>	1.87 × 10 <sup>-11</sup>	0.080
o-Xylene <sup>b</sup>	0.17 ± 0.12	(4.02 ± 2.82) × 10 <sup>9</sup>	1.36 × 10 <sup>-11</sup>	0.055
<b>Oxygenated VOC</b>				
Acetaldehyde <sup>a</sup>	2.37 ± 1.38	(5.77 ± 3.35) × 10 <sup>10</sup>	1.50 × 10 <sup>-11</sup>	0.866
MACR <sup>b</sup>	0.16 ± 0.12	(3.89 ± 2.97) × 10 <sup>9</sup>	2.90 × 10 <sup>-11</sup>	0.113
Methanol <sup>a</sup>	1.44 ± 0.81	(3.50 ± 1.96) × 10 <sup>10</sup>	9.00 × 10 <sup>-13</sup>	0.031
Acetone <sup>a</sup>	1.11 ± 0.51	(2.69 ± 1.24) × 10 <sup>10</sup>	1.80 × 10 <sup>-13</sup>	0.005
MVK <sup>b</sup>	0.28 ± 0.15	(6.72 ± 3.61) × 10 <sup>9</sup>	2.00 × 10 <sup>-11</sup>	0.134
Ethanol <sup>a</sup>	5.48 ± 3.81	(1.33 ± 0.93) × 10 <sup>11</sup>	3.20 × 10 <sup>-12</sup>	0.426
Propanol <sup>a</sup>	0.31 ± 0.21	(7.41 ± 5.15) × 10 <sup>9</sup>	5.80 × 10 <sup>-12</sup>	0.043
Butanol <sup>a</sup>	0.59 ± 0.33	(1.45 ± 0.80) × 10 <sup>10</sup>	8.50 × 10 <sup>-12</sup>	0.123

a) IUPAC preferred value; b) Atkinson and Arey (2003); \* Average of both



1 **PARADE.** For comparison, data collected with a PTR-ToF-MS (Ionicon Analytik GmbH,  
2 Austria) (described in Jordan et al. (2009)) during the PARADE field campaign, were  
3 analysed. Measurements were taken between 15 August and 9 September 2011 at the Taunus  
4 observatory on the summit of Kleiner Feldberg (50°13'25" N, 8°26'56" E) under various  
5 meteorological conditions. A detailed description of the measurement site and measurements  
6 performed during PARADE can be found in Crowley et al. (2010) and Bonn et al. (2014).  
7 The PTR-ToF-MS was operated continuously with minor interruptions. Background  
8 measurements were conducted regularly with zero air and calibration measurements were  
9 performed with a multicomponent gas standard before and after the campaign. For this study  
10 two weeks of data (21 to 27 August 2011 - Period 1; 01 to 06 September 2011 - Period 2)  
11 were selected, each with approximately the same amount of data points as the ClearLo  
12 dataset. Period 1 was mainly influenced by continental air masses and only towards the end  
13 by air that travelled over the UK and the English Channel (UK-marine). Period 2 was  
14 dominated by UK-marine air, but was also influenced by air masses that travelled over the  
15 Atlantic (see Phillips et al. (2012)).

16 **Data.** While the ClearLo data presented here were collected at an urban background site with  
17 mainly anthropogenic emissions, the PARADE campaign took part at a semi-rural site.  
18 Biogenic emissions were expected from the direct vicinity, but some anthropogenic influence  
19 was apparent from the proximity of the highly populated Rhein-Main area and Frankfurt.

20 Three mass channels were selected for the analysis corresponding to acetone/propanal,  
21 toluene and ethylbenzene/xylene. In the following, the combined signal of acetone and  
22 propanal is referred to as acetone as well as the signal of ethylbenzene and xylene is referred  
23 to as xylene for more clarity. The compounds used for analysis represent different sources of  
24 VOC. Toluene and xylene are counted along anthropogenic VOC, monoterpenes are of  
25 biogenic origin and the OVOC (acetone and methanol) are whether emitted directly or  
26 produced by photochemical oxidation in the atmosphere (Monks et al. (2009) and references  
27 therein). They were selected, because their volume mixing ratios could be determined with  
28 low uncertainty for both instruments. Aromatic compounds such as toluene and xylene are  
29 well suited for this investigation, because they often show short-term high variability. The  
30 analysis of the PARADE data also includes methanol and the sum of monoterpenes. The  
31 characteristic parameters of the measurements during ClearLo and PARADE are given in  
32 Table 2.





1 Table 2: Characteristics of the two different PTR-ToF-MS deployed during ClearfLo and  
2 PARADE. Given are the sensitivity based on normalised counts per second (ncps), accuracy  
3 as error for the measurements and the limit of detection (LOD), which was calculated as  $1\sigma$   
4 for ClearfLo and  $2.6\sigma$  for PARADE based on 1 min data.

	Compound	Sensitivity (ncps ppbV <sup>-1</sup> )	Accuracy (%)	LOD ( $1\sigma$ ) (ppbV)
ClearfLo	Acetone	9.89	18*	0.56
	Toluene	6.36	18* (22)	0.38
	Xylene	9.00	18* (20)	0.41

\* 1st column does not include effect of isobaric overlap from aromatic fragmentation, 2nd column includes estimation of isobaric overlap.

	Compound	Sensitivity (ncps ppbV <sup>-1</sup> )	Accuracy (%)	LOD ( $2.6\sigma$ ) (ppbV)
PARADE	Acetone	37.0	16	0.08
	Toluene	26.9	8	0.04
	Xylene	33.4	13	0.01
	Methanol	12.7	17	0.24
	Monoterpenes	14.1	10	0.02

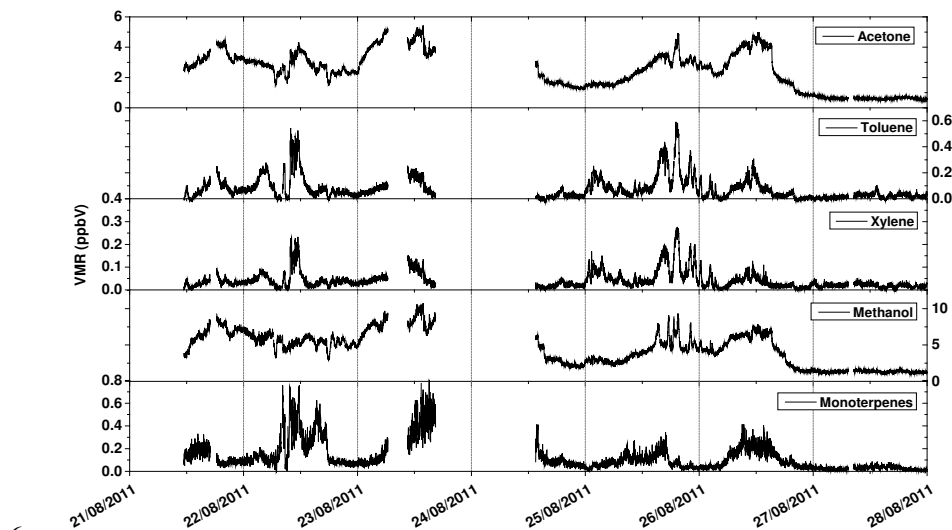
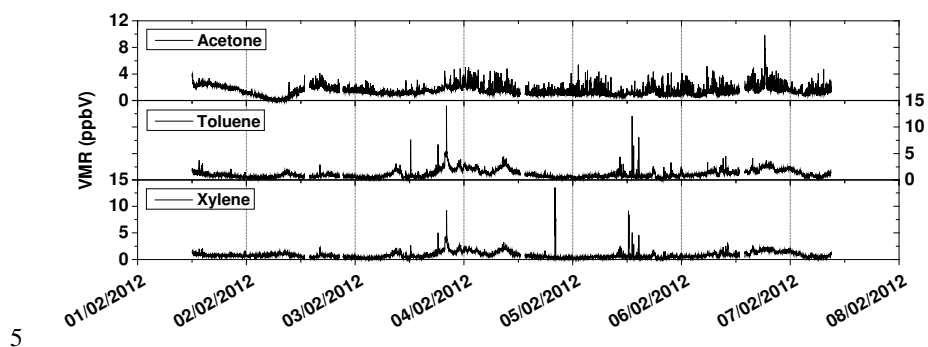
Effects of isobaric overlap from fragmentation taken into account.

5  
6 Figure 1 shows the time series of the VOC for ClearfLo (top) and PARADE Period 1  
7 (bottom). The range of mixing ratios for ClearfLo is much wider and higher mixing ratios are  
8 reached. Values for acetone show values up to a factor of 1.8 higher in ClearfLo compared to  
9 PARADE, while the aromatic compounds are two orders of magnitude higher. This  
10 emphasises the diversity of the two field sites. In the box plots, presented in Figure 2, some  
11 interesting patterns are apparent. For ClearfLo all three compounds exhibit a similar  
12 interquartile range (0.60 to 0.86 ppbV) but also very high maximum values. For PARADE a  
13 different distribution is depicted. Acetone has a wider interquartile range of 1.83 ppbV and  
14 has a higher mean value than toluene and xylene. The aromatic compounds have a much  
15 smaller range compared to ClearfLo (0.03 to 0.08 ppbV). Methanol has a wider range than  
16 acetone and the monoterpenes look similar to the aromatic compounds. Both periods of  
17 PARADE show the same pattern. The ranges of the mixing ratios during the campaigns are

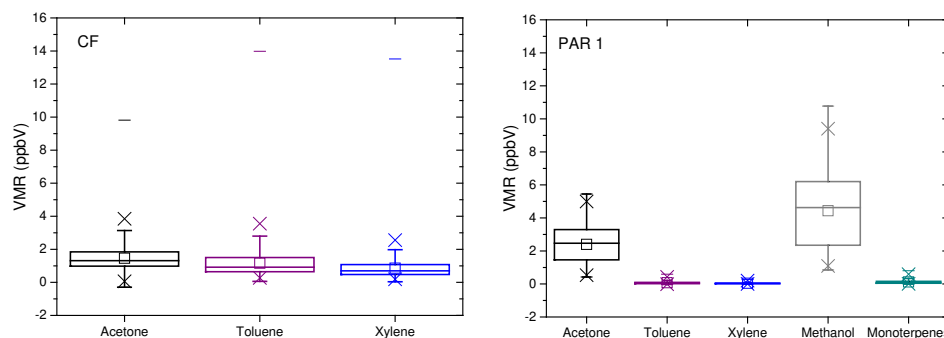


1 summarised in Table 3. Values below the limit of detection (LOD) as well as negative values  
2 are not disregarded in this analysis to preserve the full range of the data in order that they can  
3 be compared to a randomly generated dataset.

4



7 Figure 1: Time series of VOC during ClearfLo (top) and PARADE Period 1 (bottom). The  
8 time resolution is 1 min.



1  
 2 Figure 2: Box plots for ClearfLo (left) and PARADE Period 1 (right) showing the minimum,  
 3 maximum, mean ( $\square$ ), median, interquartile range (box) and percentiles at 1% and 99% ( $\times$ ).  
 4 Table 3: Overview of the range of VOC mixing ratios during ClearfLo and PARADE (PAR).

		Minimum	Maximum	Mean	Interquart. Range	Max - Min
ClearfLo	Acetone	-0.294	9.816	1.459	0.864	10.110
	Toluene	0.058	13.982	1.162	0.862	13.924
	Xylene	0.038	13.519	0.861	0.601	13.482
PAR 1	Acetone	0.426	5.447	2.400	1.833	5.021
	Toluene	-0.030	0.592	0.076	0.078	0.622
	Xylene	-0.008	0.277	0.041	0.030	0.285
	Methanol	0.851	10.775	4.438	3.858	9.923
	Monoterp.	-0.008	0.801	0.124	0.116	0.809
PAR 2	Acetone	0.544	4.873	1.987	1.797	4.329
	Toluene	-0.017	0.646	0.078	0.073	0.663
	Xylene	-0.004	0.358	0.046	0.039	0.362
	Methanol	0.781	10.649	3.776	2.739	9.869
	Monoterp.	-0.009	0.692	0.075	0.086	0.701

5  
 6  
 7

8 OH reactivity relating to the VOC under study is calculated from the first term of equation  
 9 (1). Reaction rates for acetone ( $1.8 \times 10^{-13} \text{ cm}^3 \text{ molecule}^{-1} \text{ s}^{-1}$ ), toluene ( $5.6 \times 10^{-12} \text{ cm}^3 \text{ molecule}^{-1}$



1  $\text{s}^{-1}$ ), methanol ( $9.0 \times 10^{-13} \text{ cm}^3 \text{ molecule}^{-1} \text{ s}^{-1}$ ) and  $\alpha$ -pinene ( $5.3 \times 10^{-11} \text{ cm}^3 \text{ molecule}^{-1} \text{ s}^{-1}$ ) are  
 2 taken from <http://iupac.pole-ether.fr/index.html>. The exact composition of the monoterpene  
 3 signal is not known, thus only the reaction rate of  $\alpha$ -pinene is used. For xylene the average of  
 4 the reaction rates of ethylbenzene and o-, m- and p-xylene ( $14.5 \times 10^{-12} \text{ cm}^3 \text{ molecule}^{-1} \text{ s}^{-1}$ )  
 5 (Atkinson and Arey, 2003) was applied. Table 4 summarises the minimum, maximum and  
 6 mean reactivity calculated from these VOC as described.

7

8 Table 4: Minimum, maximum and mean VOC reactivity and standard deviation calculated  
 9 from the VOC under study for ClearfLo and PARADE.

VOC reactivity ( $\text{s}^{-1}$ )		Minimum	Maximum	Mean	Stdev
CF	ATX	0.036	4.864	0.463	0.289
PAR1	ATX	0.000	0.191	0.035	0.028
	ATX+M+MT	0.026	1.296	0.292	0.205
PAR2	ATX	0.001	0.222	0.036	0.024
	ATX+M+MT	0.044	0.987	0.215	0.119

ATX: Acetone, toluene and xylene

ATX+M+MT: Acetone, toluene, xylene, methanol and monoterpenes

10

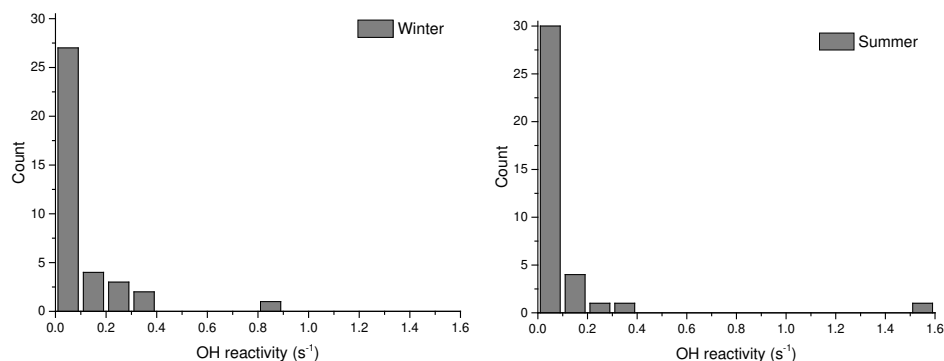
11 The time resolution of PTR-ToF-MS is only limited by the signal to noise ratio and resulting  
 12 detection limit. Both instruments were operated with a 1 min time resolution. Volume mixing  
 13 ratios of VOC were averaged over different intervals and standard deviations were derived.  
 14 An average was only included for analysis, if its data recovery was at least 50%. The OH  
 15 reactivity for each VOC was calculated and summed as required. Only the standard deviations  
 16 were propagated as errors of reactivity, as the focus of this work is on investigating VOC  
 17 variability.

18 For clarity throughout this paper the notation  $R = R_{\text{OH}}$  for reactivity regarding the OH radical  
 19 replaces  $k_{\text{OH}}$  (cf., eq. (1); see also Nölscher et al. (2012a)). Indices denote the origin of the  
 20 data (PTR = PTR-ToF-MS or GC = DC-GC-FID and CL = ClearfLo or PAR = PARADE).  
 21 Numbers indicate the averaging time in minutes. If only some VOC are taken into account for  
 22 calculating the reactivity, this will be indicated, e.g.  $R_{\text{PTR,CL}}^{\text{OVOC},5}$  is the OH reactivity calculated  
 23 from the 5 min mean concentration of acetone, measured with the PTR-ToF-MS during  
 24 ClearfLo.



## 1 2.2 VOC reactivity distribution

2 For a more general view of the factors that drive variation in VOC reactivity, its frequency  
3 distribution was investigated. GC data from the winter (9 January – 9 February 2012) and  
4 summer IOP (18 July – 19 August 2012) during ClearfLo were applied. The VOC reactivity,  
5  $R_{GC,CL}^{VOC_i}$ , was calculated for each measured  $VOC_i$  and ranged from 0.003 to 0.822  $s^{-1}$  in winter  
6 and from 0.001 to 1.568  $s^{-1}$  in summer with a total VOC reactivity of 4.010  $s^{-1}$  and 3.862  $s^{-1}$ ,  
7 respectively. The majority of  $R_{GC,CL}^{VOC_i}$  values lies below 0.1  $s^{-1}$  as can be seen from the  
8 frequency distribution plotted in Figure 3, where more than 70% of the winter and 80% of the  
9 summer data are in the first interval from 0 to 0.1  $s^{-1}$ . Seasonal differences in OH reactivity  
10 emission rates have previously been described by Nölscher et al. (2013) for measurements at  
11 a Norway spruce between spring and early autumn. Although the composition of VOC during  
12 ClearfLo changed from winter to summer, no seasonal dependency could be found in the  
13 shape of the frequency distribution for the reactivity  $R_{GC,CL}^{VOC_i}$ . In both cases  $R_{GC,CL}^{TVOC}$  is  
14 dominated by the sum of low reactivity contributions and less by single compounds with high  
15 reactivity.



16

17 Figure 3: OH reactivity,  $R_{GC,CL}^{VOC_i}$ , frequency distribution for the ClearfLo campaign in winter  
18 (left) and summer (right). Bin size is 0.1  $s^{-1}$  for both plots.

## 19 2.3 Generation of a randomized data set

20 To differentiate between pure statistical effects and measurement related characteristics, a  
21 randomized data set was produced and analysed in the same way as the PTR-ToF-MS data.  
22 The distribution of OH reactivity is skewed towards smaller values and only positive values



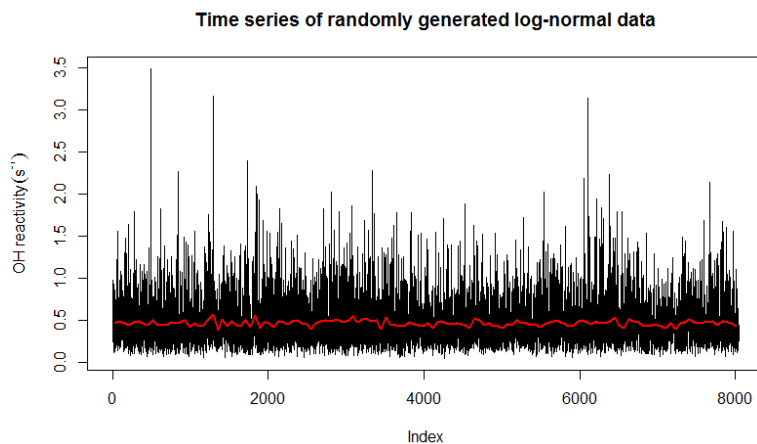
1 of OH reactivity are expected, hence it is better described by a log-normal distribution  
2 compared to a normal distribution (Limpert et al., 2001). The data set of random numbers was  
3 generated simulating an OH reactivity distribution comparable to the ClearfLo data set. The  
4 sample mean  $m = 0.463 \text{ s}^{-1}$  and standard deviation  $sd = 0.289 \text{ s}^{-1}$  from the ClearfLo 1 min  
5 dataset were used to define the parameters  $\mu$  (equation (2)) and  $\sigma$  (equation (3)) for the log-  
6 normal distribution of random numbers.

$$7 \quad \mu = \log \left( \frac{m}{\sqrt{1 + \frac{sd^2}{m^2}}} \right) \quad (2)$$

8

$$9 \quad \sigma = \sqrt{\log \left( 1 + \frac{sd^2}{m^2} \right)} \quad (3)$$

10 A log-normal distribution of a total of 8040 random numbers was generated using the `dlnorm`  
11 ( $\#, \mu, \sigma$ )-function in R. This provides a set of data comparable to 134 hours of OH reactivity  
12 measurements with a time resolution of 1 min. Figure 4 shows the random data set as a time  
13 series together with the hourly mean containing 60 data points. On observation of Figure 4, it  
14 becomes obvious that the range of the hourly average is very small with a standard deviation  
15 of  $0.034 \text{ s}^{-1}$ .



16

17 Figure 4: Time series of randomly generated log-normal data set containing 8040 numbers.

18 The "1min" data are shown in black. The average over 60 data points is plotted in red.



### 1 3 Results and Discussion

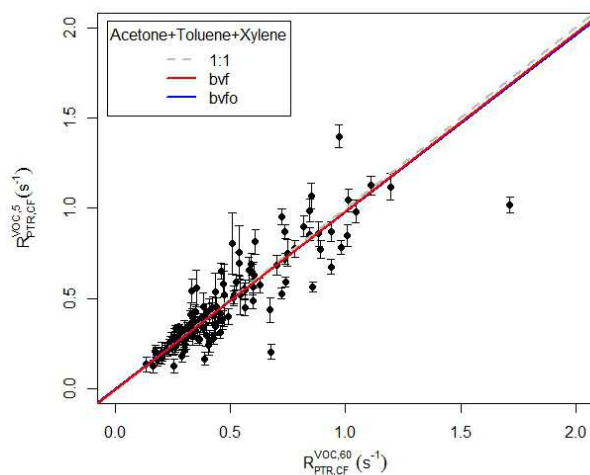
2 Initially the OH reactivity  $R_{PTR}^{VOC}$  was calculated from the PTR data for ClearfLo and  
3 PARADE. For both campaigns the signals of acetone, toluene and xylene (referred to  
4 generally as VOC) were used. The effects of differing sampling intervals on the derived  
5 reactivity were explored. For each campaign and VOC dataset a correlation of the average  
6 values of  $R_{PTR}^{VOC,t}$  for different intervals ( $t = 5, 10, 20$  and  $30$  min) against the  $60$  min average  
7  $R_{PTR}^{VOC,60}$  was calculated. The intervals are chosen to be the first  $t$  minutes of each hour to  
8 simulate the initiation of a GC sequence, thus the  $10$  min average also covers the  $5$  min  
9 averaging period and so on.

10 Figure 5 shows the linear correlation of the  $5$  min average  $R_{PTR,CL}^{VOC,5}$  versus the  $60$  min value  
11  $R_{PTR,CL}^{VOC,60}$  for the ClearfLo winter campaign. Data were fitted with a bivariate regression line  
12 with an intercept (bvfi) and forced through the origin (bvfo). The deviation from the slope of  
13 the linear regression to a unity gradient  $m_{res} = (m_{R^{<60} / R^{60}} - 1)$  is taken as a measure of how well  
14 the value of hourly OH reactivity is represented by the shorter interval average and is further  
15 referred to as the residual slope.

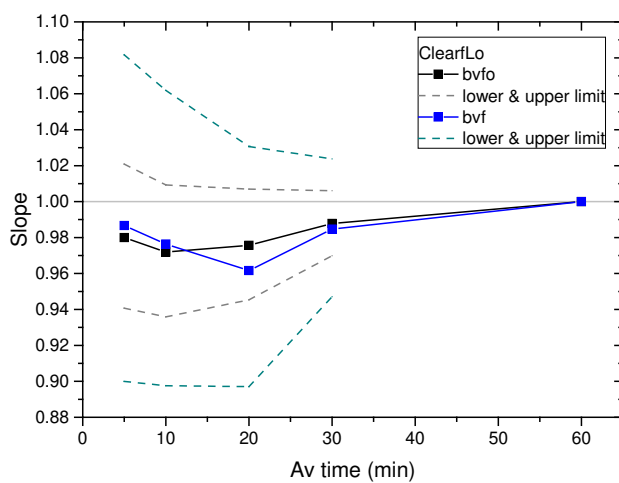
16 The slopes of both fits in Figure 5 are below  $1.0$ , indicating an under prediction of the  
17 reactivity during ClearfLo by the value calculated from the first  $5$  min of each hour. In this  
18 case there is only a small deviation ( $1.3\%$ ) from a unity gradient (see Figure 6). For all  
19 averaging intervals the slope is equal to  $1$  in the range of the uncertainties of the fit.

#### 20 3.1 Effects of different sampling intervals

21 For the different averaging intervals the difference to the hourly average  
22 ( $\Delta R = R_{PTR,CL}^{VOC,t<60} - R_{PTR,CL}^{VOC,t=60}$ ) was calculated and their standard deviations are given in Table 5  
23 as a measure of variance.  $\Delta R$  generally decreases with increasing averaging time. Also  
24 presented in Table 5 are the results from fitted Gaussian functions to the frequency  
25 distribution of the ratio of the shorter interval averages to the  $60$  min average. Bins of  $0.1$   
26 were chosen for the frequency distributions. The standard deviation of  $\Delta R$  as well as the full  
27 width at half maximum (FWHM) decrease, when averages are calculated for longer intervals.  
28 The centre of all Gaussian fits achieve  $0.99$ .



1  
2 Figure 5: Linear correlation with bivariate fit of the OH reactivity calculated from the signals  
3 of acetone, toluene and xylene for average intervals of 5 min and 60 min for ClearfLo. The  
4 standard deviation of the 5 min means are plotted as error bars.



5  
6 Figure 6: Development of the slope of the correlation of OH reactivity  $R_{PTR,CL}^{VOC,I}$  depending on  
7 the sampling interval for ClearfLo. Slopes for bvfo (black) and bvf (blue) with their lower and  
8 upper limits are shown.

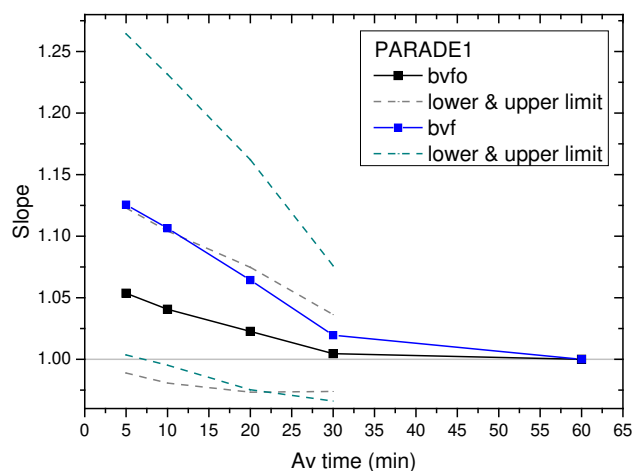




- 1 Table 5: Standard deviation of  $\Delta R$  and results from Gaussian fits of the ratio of OH reactivity  
 2  $R_{PTR,CL}^{VOC,t<60} / R_{PTR,CL}^{VOC,t=60}$  calculated from shorter interval averages to 60 min average for ClearfLo.

Notation	Time interval (min)	$\Delta R$	Gaussian Fit	
		Stdev ( $s^{-1}$ )	Centre	FWHM
$R_{PTR,CL}^{VOC,5}$	5	0.12	$0.998 \pm 0.011$	$0.337 \pm 0.025$
$R_{PTR,CL}^{VOC,10}$	10	0.12	$0.997 \pm 0.008$	$0.244 \pm 0.020$
$R_{PTR,CL}^{VOC,20}$	20	0.10	$0.988 \pm 0.006$	$0.246 \pm 0.013$
$R_{PTR,CL}^{VOC,30}$	30	0.06	$0.992 \pm 0.004$	$0.198 \pm 0.009$

- 3  
 4 For Period 1 of the PARADE data (PAR1) the results show a slope greater than 1 (Figure 7).  
 5 The high variability of the data is reflected by a higher divergence of the slopes of 1.13 for  
 6 bvfo fit and 1.05 for the bvfo fit based on 5 min averaged data. The small standard deviations  
 7 of  $\Delta R$  given in Table 6 highlight the narrow range of calculated OH reactivity  $R_{PTR,PAR1}^{VOC}$   
 8 However, the high variability of the data is reflected by the FWHM of the frequency  
 9 distributions of the ratios which is higher for each interval when compared to ClearfLo.



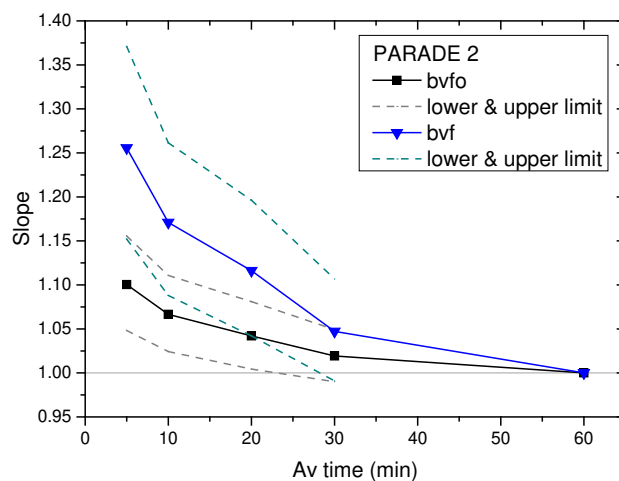
- 10  
 11 Figure 7: Development of the slope of the correlation of OH reactivity  $R_{PTR,PAR1}^{VOC,t}$  depending on  
 12 the averaging time for PARADE - Period 1.



- 1 Table 6: Standard deviation of  $\Delta R$  and results from Gaussian fits of the ratio of OH reactivity  
 2  $R_{PTR,PAR1}^{VOC,t<60} / R_{PTR,PAR1}^{VOC,t=60}$  calculated from shorter interval averages to 60 min average for PARADE  
 3 - Period 1.

Notation	Time interval (min)	$\Delta R$	Gaussian Fit	
		Stdev ( $s^{-1}$ )	Center	FWHM
$R_{PTR,PAR1}^{VOC,5}$	5	0.016	$0.980 \pm 0.011$	$0.379 \pm 0.027$
$R_{PTR,PAR1}^{VOC,10}$	10	0.015	$0.976 \pm 0.012$	$0.353 \pm 0.026$
$R_{PTR,PAR1}^{VOC,20}$	20	0.012	$0.997 \pm 0.013$	$0.310 \pm 0.030$
$R_{PTR,PAR1}^{VOC,30}$	30	0.008	$0.995 \pm 0.009$	$0.273 \pm 0.020$

- 4  
 5 For Period 2 (PAR2), an over prediction of the OH reactivity  $R_{PTR,PAR2}^{VOC}$  can be observed again  
 6 (Figure 8), but with an even greater slope of 1.26. In both periods of PARADE the slope  
 7 approaches a value of 1 as increasing averaging time is taking more of the variability within  
 8 one hour into account. Standard deviations of  $\Delta R$  and FWHM values are similar to Period 1  
 9 of the PARADE data, while the centres of the Gaussians are closer to 1 (Table 7).



- 10  
 11 Figure 8: Development of the slope of the correlation of OH reactivity  $R_{PTR,PAR2}^{VOC,t}$  depending on  
 12 the averaging time for PARADE - Period 2.



- 1 Table 7: Standard deviation of  $\Delta R$  and results from Gaussian fits of the ratio of OH reactivity  
2  $R_{PTR,PAR2}^{VOC,t<60} / R_{PTR,PAR2}^{VOC,t=60}$  calculated from shorter interval averages to 60 min average for PARADE  
3 - Period 2.

Notation	Time interval (min)	$\Delta R$	Gaussian Fit	
		Stdev ( $s^{-1}$ )	Center	FWHM
$R_{PTR,PAR2}^{VOC,5}$	5	0.013	$0.996 \pm 0.014$	$0.352 \pm 0.034$
$R_{PTR,PAR2}^{VOC,10}$	10	0.009	$0.994 \pm 0.013$	$0.296 \pm 0.031$
$R_{PTR,PAR2}^{VOC,20}$	20	0.008	$0.992 \pm 0.008$	$0.238 \pm 0.019$
$R_{PTR,PAR2}^{VOC,30}$	30	0.006	$1.010 \pm 0.004$	$0.238 \pm 0.010$

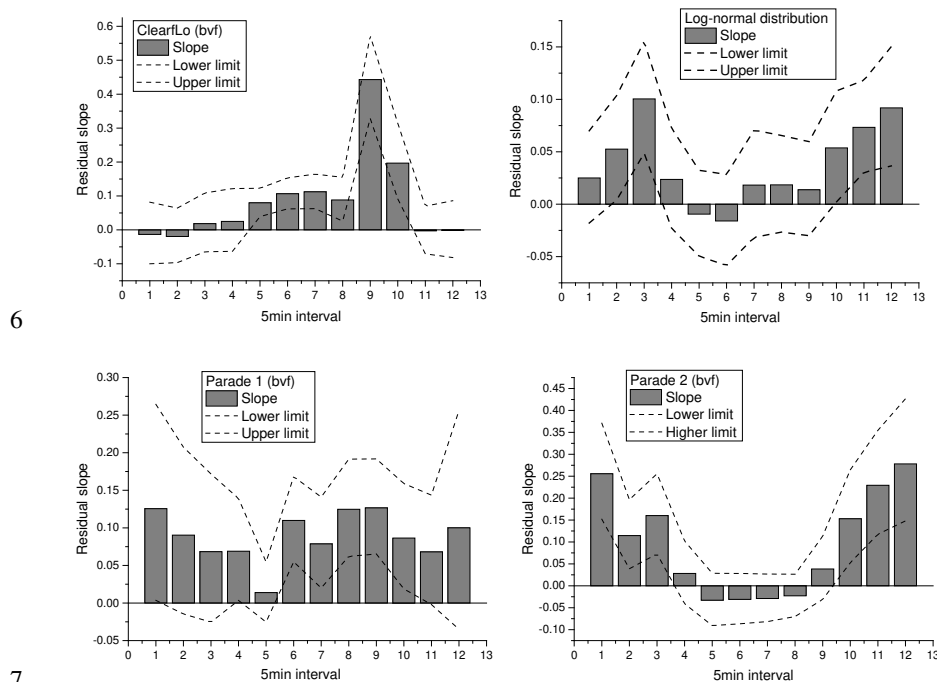
- 4  
5 When OH reactivity is calculated from GC measurements of VOC, some of the variability in  
6 the data is not captured, because air sampling alternates with the GC run itself (Hopkins et al.,  
7 2003). In this manner, the analytes are collected for a short duration which is then used to  
8 represent the whole measurement cycle. This work suggests that a discrepancy between 60  
9 min averages and shorter intervals can be caused due to the variable nature of atmospheric  
10 VOC. A sampling time of only five minutes can cause a deviation of more than 25%.  
11 Accordingly, this would then artificially contribute to missing OH reactivity.  
12 The deviation is greater for the semi-rural measurements in the Taunus during PARADE  
13 compared to the urban measurements in London. Although the range of the analysed VOC  
14 reactivity is smaller during PARADE, the highly frequent fluctuations cause a greater  
15 variability in OH reactivity for the investigated intervals.

### 16 3.2 The distribution of residual slopes across consecutive 5 min intervals

- 17 In the previous section, only reactivity calculated from the average of the first 5, 10, 20 and  
18 30 min was compared to the hourly mean. Naturally, these averages have different values,  
19 depending on the point at which they are selected from the hour under study. They may over-  
20 or under predict the hourly mean as can be seen from Figure 9 where residual bvf slopes  
21 between  $R_{PTR}^{VOC,5}$  and  $R_{PTR}^{VOC,60}$  (cf. Figure 4) are plotted for consecutive 5 min averaging periods  
22 within the hour. A tendency towards an over prediction of OH reactivity is observed for both



1 campaigns (ClearfLo - top left, PARADE – bottom) and also for the randomized data set (top  
2 right). For the randomized data set bvfo was used - bvfo has a much higher slope as the data  
3 are clustered together within a small range. On average the residuals are nearly 10% with a  
4 standard deviation of 0.1% or less ( $8.6\% \pm 0.1\%$  - for ClearfLo;  $8.85\% \pm 0.03\%$  for PARADE  
5 1;  $9.5\% \pm 0.1\%$  for PARADE 2;  $4\% \pm 4\%$  for the randomized data).



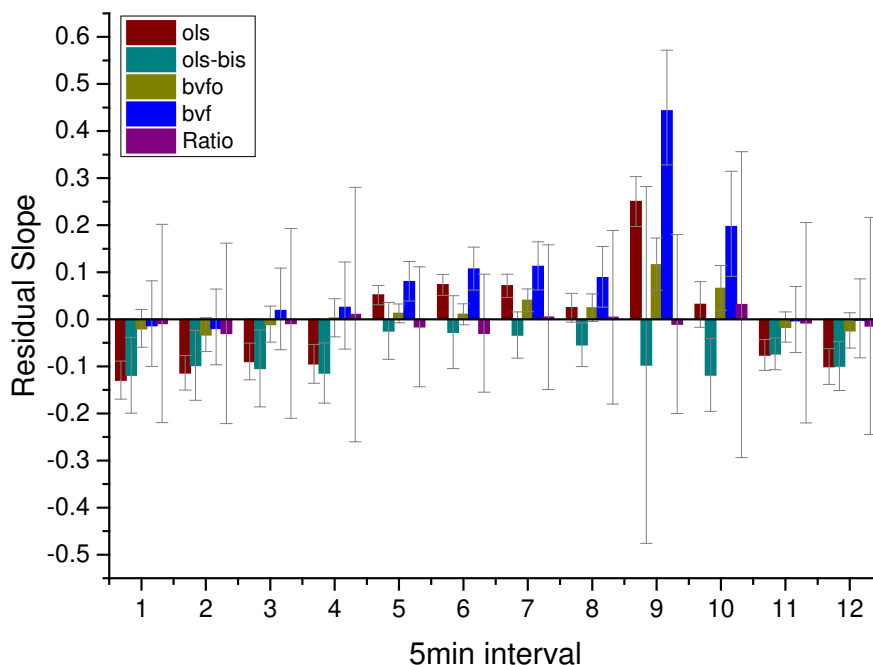
7  
8 Figure 9: Residual slopes of the correlation of all 5min means to the hourly mean.

9  
10 For linear regression the standard least squares fit is widely used. This method is less  
11 adequate when errors in both y and x are assumed or when the assignment of the independent  
12 variable is not clear (Isobe et al., 1990). Other methods for bivariate fitting in natural sciences  
13 have been discussed in the literature (Isobe et al., 1990;Warton et al., 2006;Cantrell, 2008).  
14 Cantrell (2008) found that a bivariate fit is less sensitive to outliers compared to an ordinary  
15 least squares (ols) fit. Warton et al. (2006) described the major axis (ma) and standard or  
16 reduced major axis regression (sma/rma). These methods are preferred when the agreement  
17 between two measurement techniques is investigated. For equally important deviations from  
18 the regression line in the x and y directions ma is used, while sma can be used when the scales



1 in x and y are not comparable. These two functions are implemented in the *smatr*-package in  
2 R. The *ma*-function is used to produce the bivariate regression line (*bvf*) and the bivariate  
3 regression forced through the origin (*bvfo*) in this work. In the work of Isobe et al. (1990) the  
4 ordinary least square regression, major axis and reduced major axis regression, and  
5 additionally *ols bisector* (*ols-bis*) regression, are compared. They point out that different  
6 slopes are to be expected for all the bivariate fits (*ma*, *sma*, *ols-bis*). For *ma* they find large  
7 uncertainties for the slope. To carry out a symmetrical analysis they recommend using the *ols-*  
8 *bisector* regression.

9 Figure 10 shows the residual slopes between  $R_{PTR,CL}^{VOC,5}$  and  $R_{PTR,CL}^{VOC,60}$  for consecutive 5 min  
10 intervals of the ClearfLo data using the different regression methods (*ols*, *ols-bis*, *bvfo*, *bvf*).  
11 The mean of the residual ratios (i.e., the average ratio minus 1) of  $R_{PTR,CL}^{VOC,5}$  to  $R_{PTR,CL}^{VOC,60}$  is also  
12 shown in Figure 10. The *bvfo* puts more weight onto low OH reactivity values compared to  
13 *bvf* and produces a line matching the majority of the data much better. Therefore, smaller  
14 residuals are observed compared to the *bvf*. The very small residual of the average ratio also  
15 emphasize that deviation from the ideal slope of 1 is mainly driven by outliers. The *ols-bis*  
16 regression shows a negative residual for all 5 min intervals. Mean deviations and ranges for  
17 all regression methods based on consecutive 5 min averaging periods are summarised in  
18 Table 8, where it can clearly be seen that once averaged across 12 intervals *ols* and the ratio  
19 have a negligible deviation. On average the *ols* shows the smallest deviation from the ideal  
20 slope of one, but in terms of stability across all 5 min intervals the *ols-bis* performs better.  
21 This analysis shows, that the extend of under or over predicting OH reactivity by short  
22 sampling intervals is a matter of how the data are compared to each other.



1

2 Figure 10: Residual slopes from different linear regression methods and the mean residual  
 3 ratio for all 5min intervals. Error bars depict the standard error of the slope for the ols fit, the  
 4 square root of the variance for the ols-bis and the lower and upper limit for the bvfo and bvf  
 5 fits and the standard deviation of the ratios.

6 Table 8: Summary of the statistics of the residual slopes and ratios from the comparisons of  
 7 the 5min means to their 60min means for the ClearLo data.

Method	Min	Max	Range	Mean	Stdev
ols	-0.129	0.250	0.379	-0.008	0.112
ols-bis	-0.119	-0.024	0.094	-0.080	0.036
bvfo	-0.033	0.116	0.149	0.014	0.043
bvf	-0.019	0.443	0.462	0.861	0.130
Ratio	-0.030	0.031	0.061	-0.006	0.017

8

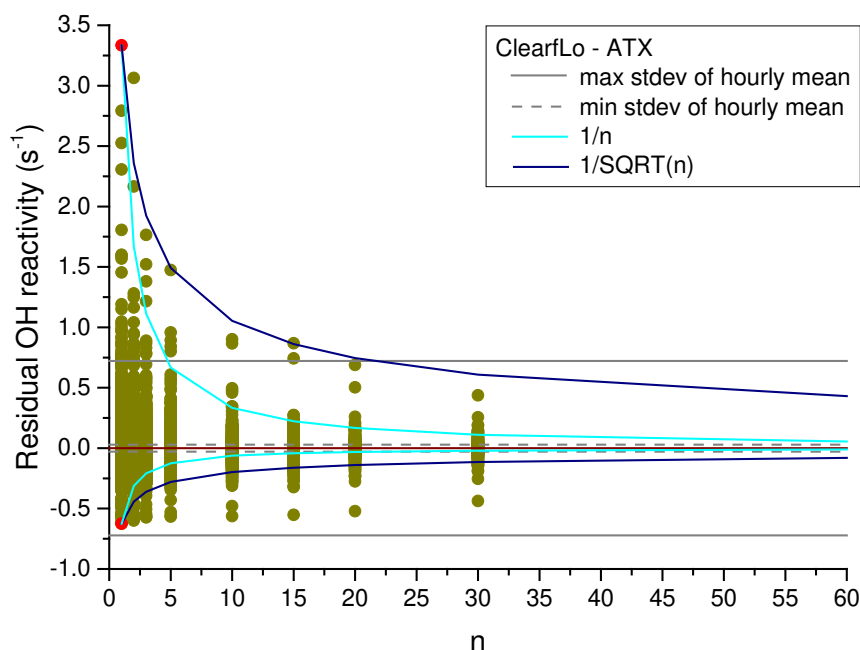
9



1 The same analysis was performed with an extended data set that included ten times the  
2 number of data points of a randomized log-normal distribution to test for any artefacts relating  
3 to the limited sample size of the PTR-ToF-MS data. No appreciable difference was obtained  
4 when compared to the smaller data set. Hence, we conclude that the observed bias to an  
5 overestimation for the bivariate fits and an underestimation for the ols-bisector regression on  
6 average is real and not an artefact caused by computing a shorter time series.

### 7 **3.3 At what sampling interval can the hourly mean be represented with a** 8 **smaller sub sample?**

9 The question being further investigated here is: how many data points are needed to calculate  
10 an average value that represents the hourly mean within its standard deviation? The ClearLo  
11 dataset of OH reactivity, based on acetone, toluene and xylene, was used to calculate 60 min  
12 means of consecutive 1 min data. Small gaps in the time series were skipped such that 60  
13 contiguous data points were computed. However, data was discarded if it included larger  
14 gaps, e.g., 1 hour or more. The set of 60 data points was further subdivided into smaller  
15 intervals to calculate means of OH reactivity  $R_{PTR,CL}^{VOC,t<60}$  of 2, 3, 5, 10, 15, 20 and 30 min.  
16 Residual reactivities for these averages were calculated by subtracting the hourly mean  
17  $R_{PTR,CL}^{VOC,60}$  before plotted against the number of data points  $n$ , which in this case corresponds to  
18 minutes (Figure 11). Corresponding standard deviations were calculated for each 60 min  
19 mean, but only the minimum and maximum values are plotted as dashed and solid grey lines  
20 in Figure 11, respectively. Additionally, two models are plotted, describing the course of the  
21 functions  $f_1$  ( $1/n$ ) (light blue) and  $f_2$  ( $1/\sqrt{n}$ ) (dark blue) starting at the maximum and  
22 minimum value (both marked as red dots). The positive range of residual OH reactivity is  
23 much wider than the negative range and is capped by the  $1/\sqrt{n}$ -function. The negative values  
24 show a slower approach to the mean. The 20 min averages all lie within the maximum  
25 standard deviation, but even when averaging over 30 min the range is much wider than the  
26 minimum standard deviation of OH reactivity.



1

2 Figure 11: Dependency of the deviation in OH reactivity from the hourly mean on the  
3 number of data points for the entire ClearfLo data set.

4 The 2, 3, 5, 10, 20 and 30min averages are now compared directly to their hourly mean and  
5 standard deviation to summarises the findings from Figure 11. As can be seen in Table 9 at  
6 20min still 2.78% of the ClearfLo data exceed their hourly mean. At 30min all data lie within  
7 the range of the standard deviation. Therefore, a sampling time greater than 20 min would be  
8 required to represent the hourly mean. The random data reach a comparable level of data  
9 exceeding the hourly mean by 2.80% for averaging over 5min only. Here, sampling for only  
10 10 min would be sufficient for representing an hour worth of data.

11

12

13

14

15

16



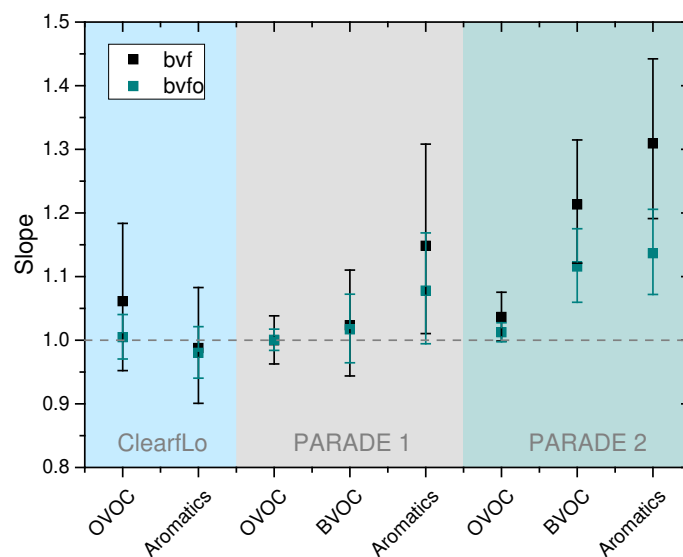


1 Table 9: Comparison to the hourly averages and their standard deviation for ClearfLo and a  
2 data set of log-normal distributed random numbers. Listed are the number and the percentage  
3 of data that exceed the stdev of the hourly mean for different n. n refers to the number of  
4 minutes that were averaged in each case.

n	ClearfLo			Random numbers		
	# data	# data > stdev	% of data > stdev	# data	# data > stdev	% of data > stdev
2	3960	838	21.16	4020	534	13.28
3	2640	457	17.31	2680	199	7.43
5	1584	225	14.20	1608	45	2.80
10	792	80	10.10	804	0	0
15	528	38	7.20	536	0	0
20	396	11	2.78	402	0	0
30	264	0	0	268	0	0

### 5 3.4 Effect of different VOC classes on OH reactivity

6 Many different atmospheric VOC have been identified (Goldstein and Galbally, 2007), all of  
7 which contribute to OH reactivity. Based on their chemical characteristics they are often  
8 divided into different classes. In order to identify how the variation of individual components  
9 contributes to the observed deviation of  $R_{PTR}^{VOC,5}$  from  $R_{PTR}^{VOC,60}$  correlations between 5 min and  
10 hourly mean reactivities were analysed for different VOC classes separately. The results are  
11 shown in Figure 12 for ClearfLo (blue area) and PARADE (grey and green areas), where  
12 OVOC contains the data from acetone for ClearfLo ( $R_{PTR,CL}^{OVOC,5}$ ) and acetone and methanol for  
13 PARADE ( $R_{PTR,PAR}^{OVOC,5}$ ). The aromatics are calculated from toluene and xylene and BVOC refers  
14 to the sum of the monoterpenes, which were only available for PARADE. Again a greater  
15 deviation from 1 is observed for the PARADE data. The OVOC show no significant deviation  
16 from 1 for both campaigns and while the aromatics are close to 1 for ClearfLo they show a  
17 significantly different value for PARADE with a deviation of up to 31%. Finally, BVOC  
18 deviate from a perfect correlation by 21% for the second period of PARADE.



1  
2 Figure 12: Bivariate fit results between 5 min averaged to 60 min averaged reactivity. Slopes  
3 are plotted for ClearfLo (blue shaded area, left) and PARADE (Period 1 – grey shaded, Period  
4 2 – green shaded, right). Correlations were analysed separately for OVOC (acetone for  
5 ClearfLo and acetone and methanol for PARADE), BVOC (monoterpenes) and aromatic  
6 compounds (toluene and xylene).

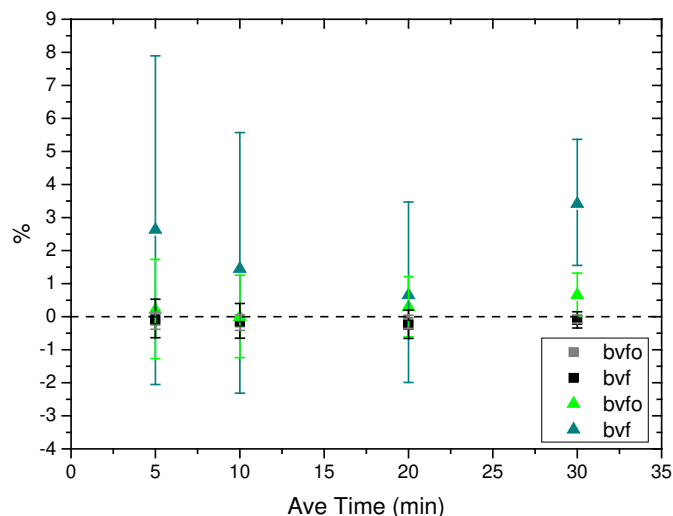
### 7 3.5 Scaling the effect to the share of VOC reactivity during ClearfLo

8 The observed deviations of the slopes from the ideal slope of 1 in Figure 12 were scaled by  
9 their share to determine the overall effect on total VOC reactivity  $R_{CL}^{TVOC}$ . Data from the same  
10 week as the PTR-ToF-MS data were used to calculate the influence of VOC speciation on OH  
11 reactivity. Over the period of 1 to 7 February 2012 the total OH reactivity of these compounds  
12 is  $R_{GC,CL}^{TVOC} = 4.05 \text{ s}^{-1}$ . Based on Table 1, OVOC contribute most to reactivity at 43%, followed  
13 by alkenes at 26% and alkanes at 21% of  $R_{GC,CL}^{TVOC}$ . The aromatic compounds have a share of  
14 6% and dienes, including isoprene, account for 3%. Finally, the contribution of the only  
15 measured alkyne is less than 1%.

16 The extend of which different VOC classes' variability effects  $R_{GC,CL}^{TVOC}$  was calculated by  
17 weighting the deviation derived from the correlations for the different classes (i.e., the  
18 deviation of the slope between  $R_{PTR,CL}^{class,5}$  and  $R_{PTR,CL}^{class,60}$  from 1) by the proportion that each class



1 contributes to the total reactivity (calculated from Table 1). Here, it is assumed that deviations  
2 derived from measurements of only a few compounds is representative of each class of VOC  
3 under study.



4

5 Figure 13: Percentage deviation in OH reactivity for different sampling intervals owing to  
6 VOC variability for the ClearLo data. Results are plotted separately for aromatic compounds  
7 (black and grey squares) and OVOC (green triangles) for both bivariate fits without (bvfo)  
8 and with an intercept (bvf). The deviations are based on the share of the VOC's class to total  
9 OH reactivity for each investigated averaging interval.

10 Based on Figure 13 5 min averages over predict VOC reactivity by up to 2.6% due to  
11 variability in OVOC concentrations. This value decreases for increasing averaging time, but  
12 shows a maximum of 3.4% for the 30 min mean. There is no significant contribution of the  
13 aromatic compounds to a deviation from the hourly mean OH reactivity for any averaging  
14 interval.

15 A similar behaviour could be expected for other classes of VOC such as the alkenes and  
16 alkanes, the second and third most important classes in Table 1. However, this could not be  
17 tested in the present study using PTR-MS data. Yet, this study shows how the effect of using  
18 short sampling intervals could account for a missing or overpredicted VOC reactivity in the  
19 range of 10% or more.



1 Lidster et al. (2014) investigated the potential increase in OH reactivity owing to higher  
2 substituted aromatic compounds, which are normally not measured in field campaigns. They  
3 state that they can contribute to up to  $0.9 \text{ s}^{-1}$  in VOC reactivity. This would increase the share  
4 of aromatic compounds by more than a factor of 3, however based on the results in  
5 Figure 13 the effect on OH reactivity would still be in the range of less than 1% while the  
6 contribution of the OVOC would only be altered slightly.  
7



#### 1 **4 Conclusions**

2 The effect of using short sampling intervals for VOC measurements on resulting OH  
3 reactivity was investigated using two different monitoring campaigns as case studies. OH  
4 reactivity was found to be both under and over predicted due to missing variability in VOC  
5 data. The divergence between OH reactivity calculated from 5 min sampling intervals and  
6 hourly values was found to be around 1 - 28% and 0 - 44% for the PARADE and ClearfLo  
7 campaigns, respectively, owing to the variability of the VOC concentrations. These  
8 discrepancies may contribute to missing OH reactivity when compared to direct  
9 measurements. Results from the urban and the semi-rural site show on average similar effects  
10 when comparing reactivity averaged over 5 min intervals to the hourly mean.

11 Comparison to a randomized data set with a similar distribution as the ClearfLo data showed  
12 that the variability of the VOC concentrations with time is the main reason for deviant results  
13 from shorter sampling intervals. For the randomized data a sampling time of less than 10  
14 min is sufficient so that all data points are within the range of the hourly standard deviation,  
15 while for the ClearfLo data it takes more than 20 min.

16 The effect of short sampling times of VOC concentrations on calculated OH reactivity is  
17 differently pronounced for each VOC class. When comparing OH reactivity calculated from  
18 VOC sampled over a 5 min period to the hourly mean, a larger divergence was found for the  
19 aromatic compounds than OVOC during ClearfLo. The same trend was observed for the  
20 PARADE campaign, while the effect of OVOC is almost negligible. Biogenic VOC, with the  
21 monoterpenes as representatives, were added for analysis. They show a similar behaviour as  
22 the OVOC, but with a slightly greater divergence.

23 The bigger proportion of measured OVOC, compared to the aromatic compounds, at the  
24 urban site during ClearfLo contributes to a higher deviation in calculated OH reactivity when  
25 using short sampling intervals. Taking the results from Lidster et al. (2014) into account, the  
26 effect of aromatic VOC increases and but is still small.

27



1

2 **Acknowledgements**

3 The authors would to thank Lis Whalley from the University of Leeds for useful comments on  
4 the manuscript. We acknowledge funding from the Natural Environment Research Council  
5 through NE/H003207/1 for ClearFlo and EU PEGASOS.

6



## 1 References

- 2 Atkinson, R., and Arey, J.: Atmospheric degradation of volatile organic compounds,  
3 Chemical Reviews, 103, 4605-4638, 2003.
- 4 Barber, S., Blake, R. S., White, I. R., Monks, P. S., Reich, F., Mullock, S., and Ellis, A. M.:  
5 Increased sensitivity in proton transfer reaction mass spectrometry by incorporation of a radio  
6 frequency ion funnel, Analytical chemistry, 84, 5387-5391, 2012.
- 7 Bohnenstengel, S. I., Belcher, S. E., Aiken, A., Allan, J. D., Allen, G., Bacak, A., Bannan, T.  
8 J., Barlow, J. F., Beddows, D. C. S., Bloss, W. J., Booth, A. M., Chemel, C., Coceal, O., Di  
9 Marco, C. F., Dubey, M. K., Faloon, K. H., Fleming, Z. L., Furger, M., Gietl, J. K., Graves,  
10 R. R., Green, D. C., Grimmond, C. S. B., Halios, C. H., Hamilton, J. F., Harrison, R. M.,  
11 Heal, M. R., Heard, D. E., Helfter, C., Herndon, S. C., Holmes, R. E., Hopkins, J. R., Jones,  
12 A. M., Kelly, F. J., Kotthaus, S., Langford, B., Lee, J. D., Leigh, R. J., Lewis, A. C., Lidster,  
13 R. T., Lopez-Hilfiker, F. D., McQuaid, J. B., Mohr, C., Monks, P. S., Nemitz, E., Ng, N. L.,  
14 Percival, C. J., Prevot, A. S. H., Ricketts, H. M. A., Sokhi, R., Stone, D., Thornton, J. A.,  
15 Tremper, A. H., Valach, A. C., Visser, S., Whalley, L. K., Williams, L. R., Xu, L., Young, D.  
16 E., and Zotter, P.: Meteorology, air quality, and health in london: The clearflo project,  
17 Bulletin of the American Meteorological Society, 96, 779-804, 10.1175/bams-d-12-00245.1,  
18 2015.
- 19 Bonn, B., Bourtsoukidis, E., Sun, T., Bingemer, H., Rondo, L., Javed, U., Li, J., Axinte, R.,  
20 Li, X., and Brauers, T.: The link between atmospheric radicals and newly formed particles at  
21 a spruce forest site in germany, Atmospheric Chemistry and Physics, 14, 10823-10843, 2014.
- 22 Cantrell, C.: Technical note: Review of methods for linear least-squares fitting of data and  
23 application to atmospheric chemistry problems, Atmospheric Chemistry and Physics, 8, 5477-  
24 5487, 2008.
- 25 Chung, M. Y., Maris, C., Krischke, U., Meller, R., and Paulson, S. E.: An investigation of the  
26 relationship between total non-methane organic carbon and the sum of speciated  
27 hydrocarbons and carbonyls measured by standard gc/fid: Measurements in the los angeles air  
28 basin, Atmospheric Environment, 37, Supplement 2, 159-170,  
29 [http://dx.doi.org/10.1016/S1352-2310\(03\)00388-1](http://dx.doi.org/10.1016/S1352-2310(03)00388-1), 2003.
- 30 Crowley, J. N., Schuster, G., Pouvesle, N., Parchatka, U., Fischer, H., Bonn, B., Bingemer,  
31 H., and Lelieveld, J.: Nocturnal nitrogen oxides at a rural mountain-site in south-western  
32 germany, Atmos. Chem. Phys., 10, 2795-2812, 2010.
- 33 Di Carlo, P., Brune, W. H., Martinez, M., Harder, H., Leshner, R., Ren, X., Thornberry, T.,  
34 Carroll, M. A., Young, V., and Shepson, P. B.: Missing OH reactivity in a forest: Evidence  
35 for unknown reactive biogenic vocs, Science, 304, 722-725, 2004.
- 36 Dolgorouky, C., Gros, V., Sarda-Estevé, R., Sinha, V., Williams, J., Marchand, N., Sauvage,  
37 S., Poulain, L., Sciare, J., and Bonsang, B.: Total oh reactivity measurements in paris during  
38 the 2010 megapoli winter campaign, Atmospheric Chemistry and Physics, 12, 9593-9612,  
39 2012.
- 40 Edwards, P., Evans, M., Furneaux, K., Hopkins, J., Ingham, T., Jones, C., Lee, J., Lewis, A.,  
41 Moller, S., and Stone, D.: Oh reactivity in a south east asian tropical rainforest during the  
42 oxidant and particle photochemical processes (OP3) project, Atmospheric Chemistry and  
43 Physics, 13, 9497-9514, 2013.



- 1 Goldstein, A. H., and Galbally, I. E.: Known and unexplored organic constituents in the  
2 earth's atmosphere, *Environmental science & technology*, 41, 1514-1521, 2007.
- 3 Hansen, R., Griffith, S., Dusanter, S., Rickly, P., Stevens, P., Bertman, S., Carroll, M.,  
4 Erickson, M., Flynn, J., and Grossberg, N.: Measurements of total hydroxyl radical reactivity  
5 during cabinex 2009—part 1: Field measurements, *Atmospheric Chemistry and Physics*, 14,  
6 2923-2937, 2014.
- 7 Hofzumahaus, A., Rohrer, F., Lu, K., Bohn, B., Brauers, T., Chang, C.-C., Fuchs, H.,  
8 Holland, F., Kita, K., and Kondo, Y.: Amplified trace gas removal in the troposphere,  
9 *Science*, 324, 1702-1704, 2009.
- 10 Hopkins, J. R., Lewis, A. C., and Read, K. A.: A two-column method for long-term  
11 monitoring of non-methane hydrocarbons (nmhcs) and oxygenated volatile organic  
12 compounds (o-vocs), *Journal of Environmental Monitoring*, 5, 8-13, 2003.
- 13 Ingham, T., Goddard, A., Whalley, L., Furneaux, K., Edwards, P., Seal, C., Self, D., Johnson,  
14 G., Read, K., and Lee, J.: A flow-tube based laser-induced fluorescence instrument to  
15 measure oh reactivity in the troposphere, *Atmospheric Measurement Techniques*, 2, 465-477,  
16 2009.
- 17 Isobe, T., Feigelson, E. D., Akritas, M. G., and Babu, G. J.: Linear regression in astronomy,  
18 *The astrophysical journal*, 364, 104-113, 1990.
- 19 Jordan, A., Haidacher, S., Hanel, G., Hartungen, E., Märk, L., Seehauser, H., Schottkowsky,  
20 R., Sulzer, P., and Märk, T.: A high resolution and high sensitivity proton-transfer-reaction  
21 time-of-flight mass spectrometer (ptr-tof-ms), *International Journal of Mass Spectrometry*,  
22 286, 122-128, 2009.
- 23 Kim, S., Guenther, A., Karl, T., and Greenberg, J.: Contributions of primary and secondary  
24 biogenic COC total OH reactivity during the cabinex (community atmosphere-biosphere  
25 interactions experiments)-09 field campaign, *Atmospheric Chemistry and Physics*, 11, 8613-  
26 8623, 2011.
- 27 Kovacs, T., Brune, W., Harder, H., Martinez, M., Simpas, J., Frost, G., Williams, E., Jobson,  
28 T., Stroud, C., and Young, V.: Direct measurements of urban oh reactivity during nashville  
29 sos in summer 1999, *Journal of Environmental Monitoring*, 5, 68-74, 2003.
- 30 Kovacs, T. A., and Brune, W. H.: Total oh loss rate measurement, *Journal of Atmospheric*  
31 *Chemistry*, 39, 105-122, 2001.
- 32 Lewis, A. C., Carslaw, N., Marriott, P. J., Kinghorn, R. M., Morrison, P., Lee, A. L., Bartle,  
33 K. D., and Pilling, M. J.: A larger pool of ozone-forming carbon compounds in urban  
34 atmospheres, *Nature*, 405, 778-781, 2000.
- 35 Lidster, R. T., Hamilton, J. F., Lee, J. D., Lewis, A. C., Hopkins, J. R., Punjabi, S., Rickard,  
36 A. R., and Young, J. C.: The impact of monoaromatic hydrocarbons on oh reactivity in the  
37 coastal uk boundary layer and free troposphere, 2014.
- 38 Limpert, E., Stahel, W. A., and Abbt, M.: Log-normal distributions across the sciences: Keys  
39 and clues on the charms of statistics, and how mechanical models resembling gambling  
40 machines offer a link to a handy way to characterize log-normal distributions, which can  
41 provide deeper insight into variability and probability—normal or log-normal: That is the  
42 question, *BioScience*, 51, 341-352, 2001.
- 43 Lou, S., Holland, F., Rohrer, F., Lu, K., Bohn, B., Brauers, T., Chang, C., Fuchs, H., Häseler,  
44 R., and Kita, K.: Atmospheric OH reactivities in the pearl river delta—china in summer 2006:





- 1 Measurement and model results, *Atmospheric Chemistry and Physics*, 10, 11243-11260,  
2 2010.
- 3 Mao, J., Ren, X., Brune, W., Olson, J., Crawford, J., Fried, A., Huey, L., Cohen, R., Heikes,  
4 B., and Singh, H.: Airborne measurement of oh reactivity during intex-b, *Atmospheric*  
5 *Chemistry and Physics*, 9, 163-173, 2009.
- 6 Mogensen, D., Smolander, S., Sogachev, A., Zhou, L., Sinha, V., Guenther, A., Williams, J.,  
7 Nieminen, T., Kajos, M., and Rinne, J.: Modelling atmospheric oh-reactivity in a boreal forest  
8 ecosystem, *Atmospheric Chemistry and Physics*, 11, 9709-9719, 2011.
- 9 Monks, P. S., Granier, C., Fuzzi, S., Stohl, A., Williams, M. L., Akimoto, H., Amann, M.,  
10 Baklanov, A., Baltensperger, U., Bey, I., Blake, N., Blake, R. S., Carslaw, K., Cooper, O. R.,  
11 Dentener, F., Fowler, D., Fragkou, E., Frost, G. J., Generoso, S., Ginoux, P., Grewe, V.,  
12 Guenther, A., Hansson, H. C., Henne, S., Hjorth, J., Hofzumahaus, A., Huntrieser, H.,  
13 Isaksen, I. S. A., Jenkin, M. E., Kaiser, J., Kanakidou, M., Klimont, Z., Kulmala, M., Laj, P.,  
14 Lawrence, M. G., Lee, J. D., Liousse, C., Maione, M., McFiggans, G., Metzger, A., Mieville,  
15 A., Moussiopoulos, N., Orlando, J. J., O'Dowd, C. D., Palmer, P. I., Parrish, D. D., Petzold,  
16 A., Platt, U., Pöschl, U., Prévôt, A. S. H., Reeves, C. E., Reimann, S., Rudich, Y., Sellegri,  
17 K., Steinbrecher, R., Simpson, D., ten Brink, H., Theloke, J., van der Werf, G. R., Vautard,  
18 R., Vestreng, V., Vlachokostas, C., and von Glasow, R.: Atmospheric composition change –  
19 global and regional air quality, *Atmospheric Environment*, 43, 5268-5350,  
20 <http://dx.doi.org/10.1016/j.atmosenv.2009.08.021>, 2009.
- 21 Nölscher, A., Williams, J., Sinha, V., Custer, T., Song, W., Johnson, A., Axinte, R., Bozem,  
22 H., Fischer, H., and Pouvesle, N.: Summertime total OH reactivity measurements from boreal  
23 forest during humppa-copec 2010, *Atmospheric Chemistry and Physics*, 12, 8257-8270,  
24 2012a.
- 25 Nölscher, A. C., Sinha, V., Bockisch, S., Klüpfel, T., and Williams, J.: Total OH reactivity  
26 measurements using a new fast gas chromatographic photo-ionization detector (gc-pid),  
27 *Atmos. Meas. Tech.*, 5, 2981-2992, 10.5194/amt-5-2981-2012, 2012b.
- 28 Nölscher, A. C., Bourtsoukidis, E., Bonn, B., Kesselmeier, J., Lelieveld, J., and Williams, J.:  
29 Seasonal measurements of total oh reactivity emission rates from norway spruce in 2011,  
30 *Biogeosciences*, 10, 4241-4257, 2013.
- 31 Phillips, G., Tang, M., Thieser, J., Brickwedde, B., Schuster, G., Bohn, B., Lelieveld, J., and  
32 Crowley, J.: Significant concentrations of nitril chloride observed in rural continental europe  
33 associated with the influence of sea salt chloride and anthropogenic emissions, *Geophysical*  
34 *Research Letters*, 39, 2012.
- 35 Ren, X., Harder, H., Martinez, M., Leshner, R. L., Oligier, A., Shirley, T., Adams, J., Simpas, J.  
36 B., and Brune, W. H.: HO<sub>x</sub> concentrations and OH reactivity observations in new york city  
37 during pmtacs-ny2001, *Atmospheric Environment*, 37, 3627-3637, 2003a.
- 38 Ren, X., Harder, H., Martinez, M., Leshner, R. L., Oligier, A., Simpas, J. B., Brune, W. H.,  
39 Schwab, J. J., Demerjian, K. L., and He, Y.: OH and HO<sub>2</sub> chemistry in the urban atmosphere  
40 of new york city, *Atmospheric Environment*, 37, 3639-3651, 2003b.
- 41 Ren, X., Brune, W. H., Oligier, A., Metcalf, A. R., Simpas, J. B., Shirley, T., Schwab, J. J.,  
42 Bai, C., Roychowdhury, U., and Li, Y.: OH, HO<sub>2</sub>, and HO<sub>x</sub> reactivity during the pmtacs-ny  
43 whiteface mountain 2002 campaign: Observations and model comparison, *Journal of*  
44 *Geophysical Research: Atmospheres* (1984–2012), 111, 2006.



- 1 Sadanaga, Y., Yoshino, A., Watanabe, K., Yoshioka, A., Wakazono, Y., Kanaya, Y., and  
2 Kajii, Y.: Development of a measurement system of oh reactivity in the atmosphere by using  
3 a laser-induced pump and probe technique, *Review of Scientific Instruments*, 75, 2648-2655,  
4 2004.
- 5 Sadanaga, Y., Yoshino, A., Kato, S., and Kajii, Y.: Measurements of oh reactivity and  
6 photochemical ozone production in the urban atmosphere, *Environmental science &  
7 technology*, 39, 8847-8852, 2005.
- 8 Shirley, T., Brune, W., Ren, X., Mao, J., Leshner, R., Cardenas, B., Volkamer, R., Molina, L.,  
9 Molina, M. J., and Lamb, B.: Atmospheric oxidation in the mexico city metropolitan area  
10 (mcma) during april 2003, *Atmospheric Chemistry and Physics*, 6, 2753-2765, 2006.
- 11 Sinha, V., Williams, J., Crowley, J., and Lelieveld, J.: The comparative reactivity method—a  
12 new tool to measure total oh reactivity in ambient air, *Atmospheric Chemistry and Physics*, 8,  
13 2213-2227, 2008.
- 14 Sinha, V., Williams, J., Lelieveld, J., Ruuskanen, T., Kajos, M., Patokoski, J., Hellen, H.,  
15 Hakola, H., Mogensen, D., and Boy, M.: Oh reactivity measurements within a boreal forest:  
16 Evidence for unknown reactive emissions, *Environmental science & technology*, 44, 6614-  
17 6620, 2010.
- 18 Thalman, R., Baeza-Romero, M., Ball, S., Borrás, E., Daniels, M., Goodall, I., Henry, S.,  
19 Karl, T., Keutsch, F., and Kim, S.: Instrument inter-comparison of glyoxal, methyl glyoxal  
20 and no 2 under simulated atmospheric conditions, *Atmospheric Measurement Techniques  
21 Discussions*, 7, 8581-8642, 2014.
- 22 Warton, D. I., Wright, I. J., Falster, D. S., and Westoby, M.: Bivariate line-fitting methods for  
23 allometry, *Biological Reviews*, 81, 259-291, 2006.
- 24 Whalley, L., Edwards, P., Furneaux, K., Goddard, A., Ingham, T., Evans, M., Stone, D.,  
25 Hopkins, J., Jones, C. E., and Karunaharan, A.: Quantifying the magnitude of a missing  
26 hydroxyl radical source in a tropical rainforest, *Atmospheric Chemistry and Physics*, 11,  
27 7223-7233, 2011.
- 28 Yoshino, A., Sadanaga, Y., Watanabe, K., Kato, S., Miyakawa, Y., Matsumoto, J., and Kajii,  
29 Y.: Measurement of total OH reactivity by laser-induced pump and probe technique—  
30 comprehensive observations in the urban atmosphere of tokyo, *Atmospheric Environment*, 40,  
31 7869-7881, 2006.
- 32  
33